LANGMUIR Article
Cite This: Langmuir XXXX, XXX, XXX−XXX
pubs.acs.org/Langmuir

Negative Dipole Potentials and Carboxylic Polar Head Groups Foster the Insertion of Cell-Penetrating Peptides into Lipid Monolayers

Matías A. Via,[‡,§] Mario G. Del Pópolo,[§] and Natalia Wilke*[,∥,⊥]

[§]CONICET & Facultad de Ciencias Exactas y Naturales, Universidad Nacional de Cuyo, Mendoza, Argentina
[‡]Instituto de Histología y Embriología de Mendoza (IHEM-CONICET) & Facultad de Ciencias Médicas, Universidad Nacional de Cuyo, Argentina
[∥]Departamento de Química Biológica Ranwel Caputto, Facultad de Ciencias Químicas, and [⊥]Centro de Investigaciones en Química Biológica de Córdoba (CIQUIBIC), Universidad Nacional de Córdoba, X5000HUA Córdoba, Argentina

Supporting Information

ABSTRACT: Cell-penetrating peptides (CPPs) are polycationic sequences of amino acids recognized as some of the most effective vehicles for delivering membrane-impermeable cargos into cells. CPPs can traverse cell membranes by direct translocation, and assessing the role of lipids on the membrane permeation process is important to convene a complete model of the CPP translocation. In this work, we focus on the biophysical basis of peptide−fatty acid interactions, analyzing how the acid−base and electrostatic properties of the lipids determine the CPP adsorption and incorporation into a Langmuir monolayer, focusing thus on the first two stages of the direct translocation mechanism. We sense the binding and insertion of the peptide into the lipid structure by measuring the changes in the surface pressure, the surface potential, and the reflectivity of the interface. We show that, beyond the presence of anionic moieties, negative dipole potentials and carboxylic polar head groups significantly promote the insertion of the peptide into the monolayer. On the basis of our results, we propose the appearance of stable CPP−lipid complexes whose kinetics of formation depends on the length of the lipids' hydrocarbon chains.

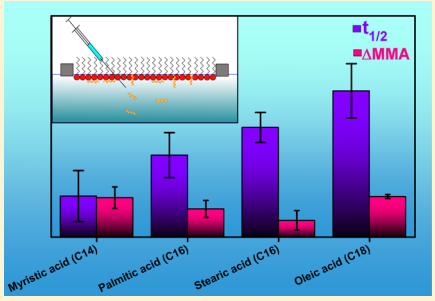

INTRODUCTION

Cell-penetrating peptides (CPPs) constitute a family of small peptides, rich in basic amino acids such as arginine and lysine, that are able to traverse cell membranes either on their own or attached to small cargoes.[1−3] CPPs are efficient vectors for introducing proteins, nucleic acid strands, nanoparticles, and fluorescent probes into the cell's cytoplasm,[4−9] and unveiling the details of how this happens is hailed as an important milestone in biophysics and other fields, where CPPs are used as cargo delivery systems. The membrane permeation mechanisms exploited by CPPs have been described previously[3,9−12] and include the standard endocytic pathway and the process of passive diffusion, or translocation, across the bilayer. In the present work, we focus on passive diffusion, as some of the molecular details behind this mechanism are still open to question and deserve close inspection. In particular, controlling the factors that regulate the energetics of CPP's translocation across biomembranes may allow to favor passive diffusion in detriment of the more cumbersome and energy-consuming endocytic pathway.

Several studies have underlined the role of interfacial electrostatics on the CPP transport.[13−16] For example, Rothbard et al. and Terrone at al.[17,18] have shown that the transmembrane electrostatic potential can, under certain circumstances, modulate the permeation rate of the peptides, whereas a number of papers have reported that the presence of negatively charged lipids in the bilayer significantly promotes membrane binding and translocation.

Apart from electrostatics, the influence of mechanical properties of the membrane,[19] of the spontaneous curvature,[18] and of the lipid flip-flop[20] on CPPs translocation have also been investigated. Furthermore, not only general membrane properties appear to be important for the peptide−membrane interactions, but also specific lipid−residue interactions may be relevant, such as ligand−receptor complex formation.[21,22] In connection with this, Herce et al.[21] have recently reported the formation of complexes between CPPs and fatty acids in a biphasic extraction system composed of water and octanol. At pHs where fatty acids were mostly dissociated, the CPP−lipid complexes were stable and readily soluble in the organic phase, encouraging the idea that these aggregates could facilitate the passive permeation of CPPs across cell membranes, which normally contain fatty acids. In addition, Herce et al. went one step forward and showed that exposing the living cells to a CPP, with prior incubation with oleic acid (OA), favored peptide intake at relatively high pHs, suggesting that the pH difference across the membrane and the presence of fatty acids in the bilayer regulates the binding to the membrane and favor the translocation process.

Received: November 24, 2017
Revised: January 27, 2018
Published: February 2, 2018

DOI: 10.1021/acs.langmuir.7b04038
Langmuir XXXX, XXX, XXX−XXX

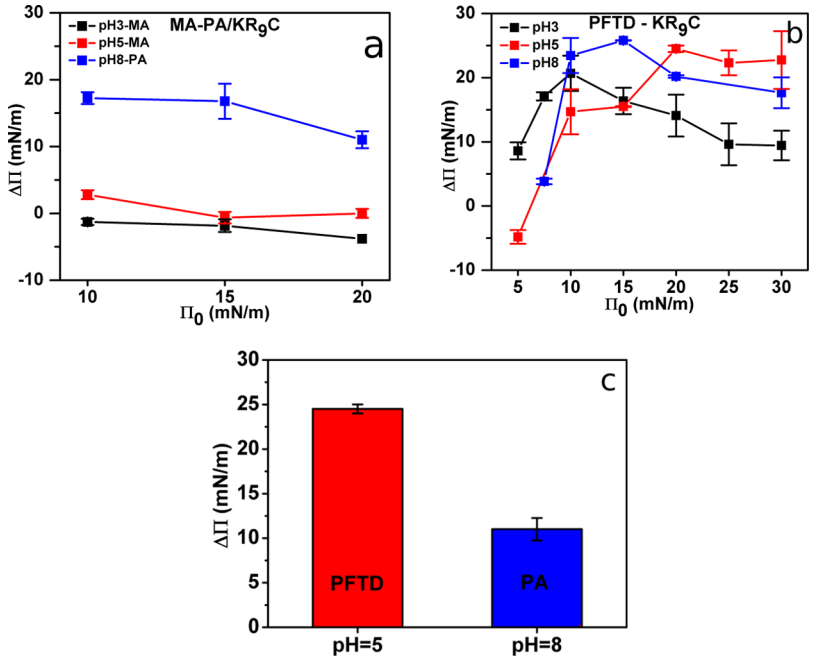

Figure 1. $\Delta\Pi$ vs Π_0 for (a) MA and PA, and (b) PFTD. (c) $\Delta\Pi$ produced in PFTD (red) and in PA (blue) monolayers, at an initial surface pressure of 20 mN/m. The results are the average of three independent experiments ± SD.

In the present work, we aim at contributing to the comprehension of the peptide−fatty acid interaction, focusing on the case where the fatty acid forms an organized film. We analyze and discuss the effect of the amphiphiles' dipole potential and of the degree of ionization of the carboxylate groups, on the adsorption and incorporation of the polyarginine into one of the membrane leaflets. We used a nona-arginine peptide, widely known as CPP,[23−27] that also includes in its sequence a lysine and cysteine residues, which allow to bind the polyarginine to proteins (lysine residue) and to gold surfaces (cysteine residue), thus allowing its use in a variety of applications. We resort to Langmuir monolayers as a model of a cell membrane and sense the binding and insertion of the peptide into the lipid structure by measuring changes in the surface pressure, the interfacial electrostatic potential, and the reflectivity of the interface. The dipole potential of the lipids depends on the composition of the acyl chain, as well as on the head group and its ionization degree.[28,29] By comparing the behavior of hydrogenated and fluorinated fatty acids that show opposing dipole potentials, we assess the effect of this parameter on the extent and kinetics of incorporation of CPP into the monolayer. Additionally, to gain deeper insights into the effect of the anionic head groups on the binding and incorporation of the polyarginine, the pH of the subphase was varied, and the incorporation into neutral and ionized fatty acid was compared with that in anionic phosphoglycerol monolayers.

EXPERIMENTAL SECTION

Materials. KR_9C(Lys−Arg_9−Cys), with a purity of ≥95%, was purchased from Innovagen (Sweden). Perfluorotetradecanoic acid (PFTD), myristic acid (MA), palmitic acid (PA), stearic acid (SA), OA, and NaCl were obtained from Sigma-Aldrich (USA). $CaCl_2$ was purchased from Merck. 1,2-Dimyristoyl-*sn*-glycero-3-phospho-*rac*-(1-glycerol) (DMPG) sodium salt was obtained from Avanti Polar Lipids (USA). Dextran sulfate (DS) sodium salt of high sulfate content (extracted from *Leuconostoc* spp, 16−20%, M_w ~6.500−10.000 Da, HDS) and chloroform were purchased from Sigma-Aldrich. Peptide and subphase solutions were prepared using deionized water with a resistivity of ~18.5 MΩ cm and filtered with an Osmoion system (Apema, BA, Argentina).

Surface Pressure Measurements. Surface pressure measurements of Langmuir monolayers were performed on a homebuilt trough (1 mL). The trough was first filled with a saline subphase (NaCl 150 mM) whose pH was previously adjusted by adding appropriate amounts of HCl or NaOH (Sigma-Aldrich). In the case of measurements performed at pH 8, a Tris buffer was used to prevent the acidification of the solution caused by the dissolution of CO_2 from air. A chloroformic lipid solution was then spread, drop by drop, onto the subphase until the desired initial surface pressure, Π_0, as measured with a KSV instrument (Finland) based on the Wilhelmy method was reached. Following solvent evaporation (5 min), an aliquot of the peptide solution was injected in the subphase through a hole on the wall of the trough. The final concentration of the peptide was 10 μM, as this concentration was previously found to be the minimum necessity to saturate the incorporation of KR_9C into a PFTD monolayer (see Figure S1). The time evolution of the surface pressure was registered after the addition of the peptide and its final value, Π_f, was determined from the asymptote of the curve. The change in surface pressure was defined as $\Delta\Pi = \Pi_f - \Pi_0$. All of the experiments were performed at 25 °C.

Surface Potential Measurements. For the pure lipid monolayers, the vibrating plate condenser method[29] was used to measure the surface potential $\Delta\Phi$ (KSV, Finland). Briefly, one electrode was placed into the aqueous subphase, whereas the second (grounded) electrode was placed and vibrated in the air at about 5 mm from the interface. The lipid film was compressed by two hydrophobic barriers at a rate of 5 mm/min, on a 200 mL volume trough at 25 °C. When measuring $\Delta\Phi$ after injecting the peptide, a homebuilt air-ionizing ^{241}Am electrode was placed at 5 mm above the subphase, whereas the reference Ag/AgCl/Cl^- electrode was submerged in the subphase. These experiments were performed on a 700 μL trough at 25 °C.

Relative Reflectivity Measurement. A black homebuilt trough (700 μL) placed on the stage of a Nanofilm EP3 Imaging Ellipsometer (Accurion, Goettingen, Germany) was used in the Brewster angle microscopy (BAM) mode, with both the analyzer and incident polarizers at an angle of zero. First, the calibration of the microscope was carried out on the bare aqueous interface with λ = 532 nm laser, reaching the sample at the experimentally calibrated Brewster angle

DOI: 10.1021/acs.langmuir.7b04038
Langmuir XXXX, XXX, XXX−XXX

(~53.1°). Subsequently, the lipid films were seeded on top of the water surface as already described. The resulting images were homogeneous in all cases. Levels of gray were registered before and after injecting the CPP in the subphase. The reflectivity of the lipid monolayer on a NaCl 0.15 M solution was considered as the base line, and all measurements recorded after the injection of the peptide were referred to this initial value (relative reflectivity). All of these experiments were performed at 25 °C and pH 5.

RESULTS AND DISCUSSION

pH and Dipole Potential Modulate the Incorporation of the Peptide into Fatty Acid Monolayers. The binding and incorporation of a solute into a Langmuir monolayer is regulated by, and in turn determines, relevant interfacial properties such as the level of compactness and phase state of the amphiphiles, the dissociation degree of titrable groups, and the interfacial electrostatic potential. We first investigated the effect of surface pressure and pH on the incorporation of KR_9C into monolayers made of MA, its fluorinated counterpart PFTD, and PA. The acyl chain of MA and PFTD is equally long (C14), but the presence of fluorine atoms in the latter leads to monolayers with negative surface potentials.[30] PA (C16) was included in the analysis with the aim of considering the insertion of the peptide into a fully charged fatty acid monolayer, conditions that could not be met with MA as this compound did not lead to stable monolayers at high pH. Compression isotherms (surface pressure and surface potential vs mean molecular area) for all of the systems investigated are shown in Figures S2−S4 of the Supporting Information.

We spread monolayers of these lipids on the air/water interface up to different surface pressure values (Π_0), and, after allowing for equilibration, the peptide was injected in the subphase in a final concentration of 10 μM. The time evolution of the surface pressure after the peptide injection was recorded until a plateau, Π_f, was reached. The change in the surface pressure of the film induced by the peptide was defined as $\Delta\Pi = \Pi_f - \Pi_0$. Figure S5 shows the $\Pi(t)$ trace for two representative experiments. In general, an increase in the surface pressure ($\Delta\Pi > 0$) indicates that the peptide induces a structural change in the monolayer and, if the value of $\Delta\Pi$ is substantial, the peptide is likely to be inserted into the monolayer.[31,32] It is important to mention that in the absence of a lipid monolayer (i.e., adsorption on a clean interface), the surface pressure of the interface remained zero for at least 1 h, after injection of the peptide, indicating that the CPP did not act as a surfactant.

Figures 1a,b shows the dependence of $\Delta\Pi$ on Π_0 at different pH values. Π_0 determines the initial lipid density and packing. Panel (a) focuses on hydrogenated fatty acids and panel (b) on PFTD. As observed, a general increase in the surface pressure was detected when the peptide was added to the subphase, pointing to the insertion of the CPP into the monolayers. The extent of surface pressure change, however, was modulated by film properties.

Figure 1a shows that $\Delta\Pi$ increases systematically when going from pH 3 to pH 8, taking the positive values at pH 5 and 8 and almost zero or slightly negative ones at pH 3. The latter may be ascribed to the instability of the MA monolayer, with the concomitant escape of the molecules to the subphase. The pattern of incorporation of the CPP into the lipid films can be readily ascribed to the ionization degree of the carboxylate moiety of the fatty acids. In this sense, the pK_a of soluble carboxylic acids lies in the range of 4−5, depending on the length of the hydrocarbon chain. For fatty acids in solution, a bulk value close to 4.8 has been reported.[33] However, when molecules form supramolecular aggregates, the pK_a shifts toward neutrality because of intermolecular interactions and confinement effects. For instance, a shift to 5.6 has been reported in the case of SA.[34] Moreover, near a charged surface, the pH is usually lower than that in bulk, further shifting the apparent pK_a of acidic amphiphiles.[33] Such an effect is more marked at low ionic strengths[35] and weakens as the ionic strength and as the mean molecular area of the monolayer increases.[36] An apparent pK_a of 7.6 has been reported for SA monolayers at low ionic strength and high packings.[37]

Therefore, at the salt concentration employed in our experiments, the pK_a values in the range of 5.6−7.6 can be expected, with shifts in the degree of ionization of the lipids from values close to zero at pH 3 to 0−50% at pH 5, and higher ionization degrees at pH 8. Arginine has a pK_a of 12, and it is safe to assume that the peptide is fully charged under all of the experimental conditions explored. With these considerations in mind, the overall interpretation of the data reported in Figure 1a is that KR_9C penetrates to a greater extent into charged monolayers, as indicated by the larger values of $\Delta\Pi$ measured at pH 8. It must be noticed, however, that the data points collected at pH 8 were obtained from PA (C16) monolayers, at variances with those at pH 3 and 5 that were measured on MA (C14). This change in the fatty acid chain length though is not responsible for the increase in $\Delta\Pi$ when pH increases, as can be judged from Figure S6, where we plot $\Delta\Pi$ (at Π_0 = 10 mN/m), as a function of pH. The peptide induced a surface pressure increment of 12 mN/m in the PA monolayer when the pH went from 5 to 8, and we would expect a similar trend for MA, should this monolayer be stable at pH 8.

The hydrogenated fatty acid monolayers showed little dependence of $\Delta\Pi$ on Π_0, suggesting a subtle dependence of the peptide insertion extent on the film packing, which is in contrast with the pronounced slope commonly observed in other systems.[38−41] The cutoff value (extrapolated Π_0 for which $\Delta\Pi$ is zero) is larger than the collapse pressure of the fatty acid monolayers, suggesting that if the fatty acids were stabilized at the interface by mixing with other lipids, the peptide would be able to penetrate the monolayer at surface pressures as high as those in which lipid monolayers are comparable to lipid bilayers (i.e., 30 mN/m or higher[42]).

Figure 1b evidences the incorporation of KR_9C into PFTD monolayers. Two main features distinguish this plot from Figure 1a. First, the values of $\Delta\Pi$ are higher in PFTD than in PA or MA, even at the lowest pH investigated; and second, $\Delta\Pi$ shows a maximum as a function of Π_0. The first observation is readily explained considering that the substitution of hydrogen atoms by fluorine decreases the pK_a of the molecule,[30] so the dissociation degree of PFTD is already larger than zero at pH 3, where MA and PA are still neutral. The second observation requires a more thorough analysis, which is provided in the following paragraphs.

First of all, to assess the ionization degree of PFTD at the studied pHs, we plotted the surface pressure corresponding to the liquid-expanded to liquid-condensed phase transition as a function of pH (see Figure S7). This parameter is expected to be constant if the degree of ionization remains unchanged and to increase as the molecules ionize. From this plot, we conclude that PFTD monolayers are completely ionized at pH 8, mostly ionized at pH 5, and only partially charged (less than 50%) at

DOI: 10.1021/acs.langmuir.7b04038
Langmuir XXXX, XXX, XXX−XXX

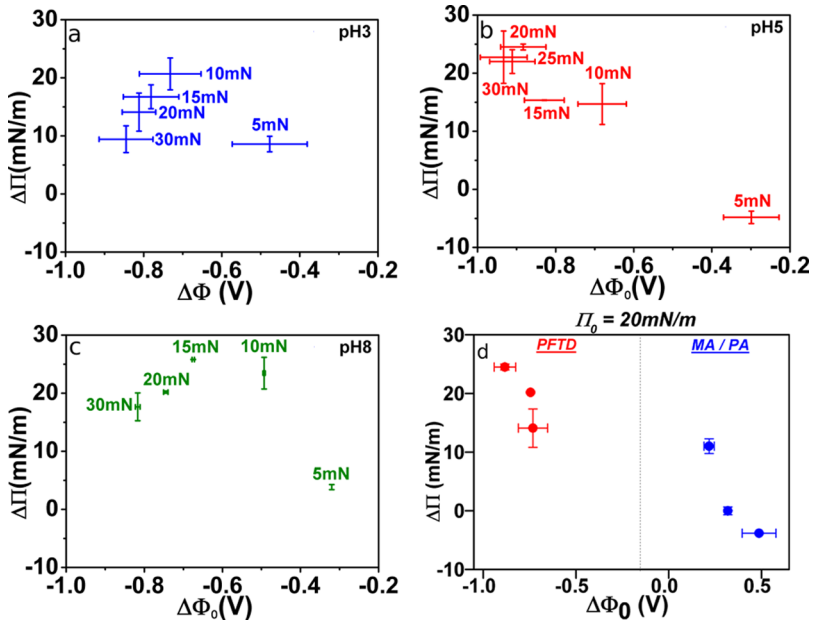

Figure 2. ΔΠ vs ΔΠ for KR_9C interacting with a PFTD film on a subphase of NaCl 150 mM at (a) pH 3, (b) pH 5, and (c) pH 8. All experiments were performed at T = 25 °C. (d) ΔΠ as function of $\Delta\Phi_0$ for an initial surface pressure of 20 mN/m, for PFTD, MA, and PA. The results are the average of three independent experiments ± SD.

pH 3. Therefore, the degree of ionization of PFTD at pH 3 (or 5) is comparable to that of MA or PA at pH 5 (or 8).

To make a more transparent and direct comparison between hydrogenated and fluorinated fatty acids, Figure 1c shows the values of ΔΠ for PA at pH 8 and for PFTD at pH 5. Remembering that at these pHs, both monolayers bear similar surface charges, we conclude that KR_9C induces larger surface pressure changes in PFTD than in PA monolayers, and we hypothesize that this is because of the inverted surface potential of PFTD, as compared to PA or MA. Following this hypothesis, we further analyzed the influence of the initial surface potential on the incorporation of the CPP into the monolayers.

Figure 2a–c shows the values for ΔΠ, extracted from Figure 1b, plotted as a function of the initial surface potentials, $\Delta\Phi_0$, at each pH. Alike the $\Delta\Pi-\Pi_0$ relation, ΔΠ shows a nonmonotonic dependence on $\Delta\Phi_0$, indicating the existence of an optimum condition for the incorporation of the CPP into the monolayer. The nonmonotonic behavior of ΔΠ can be explained in terms of two opposing factors: the incorporation of the peptide is favored in films with low densities and with high negative surface potentials.

To shed more light on the effect of surface potential, in Figure 2d, we show the variation of ΔΠ with $\Delta\Phi_0$ for all the systems investigated, at an initial Π_0 of 20 mN/m, which is the maximum surface pressure at which all systems can be compared. In this figure, each data point corresponds to a different condition (different lipid or different pH). In spite of this, a clear decrease in ΔΠ as $\Delta\Phi_0$ increases can be observed, pointing out that the surface potential of the monolayer is an important regulator for the peptide insertion. In connection with this, positive dipole potentials are known to favor the partition of anions inside lipid bilayers.[43] Here, we report the opposite phenomenon; cationic peptides incorporate into monolayers more easily if the dipole potential is negative. Regarding the PFTD monolayer, its surface potential gets more negative as the film is compressed (see Figure S2, for example); thus both parameters change in opposite directions, which leads to optimal penetration conditions at intermediate film packings.

The maximum value of $\Delta\Pi^m$ is plotted as a function of pH in Figure 3, where the corresponding values of initial surface pressure, Π_0^m, and interfacial potential, $\Delta\Phi^m$, are overlaid. Π_0^m changes with the pH, being smaller at pH 3, when the PFTD monolayers are more stiff (see Figure S7) because of partial neutralization of the molecules. Therefore, the incorporation of the CPP is maximal at lower initial surface pressures (Figure 2), and the final surface pressure reached is lower. At pH 5 and 8, the compression isotherms are similar (Figure S2). However, the surface potential is more negative at pH 5 (Figure S8), leading to a higher value of Π_0^m and of final surface pressures.

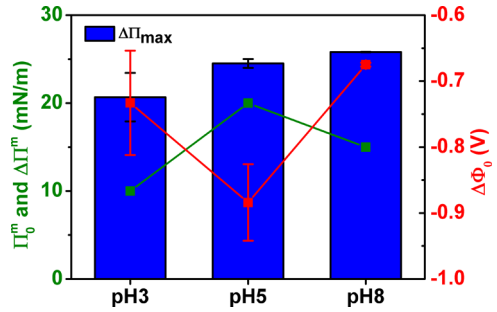

Figure 3. Surface pressure change, $\Delta\Pi^m$, associated to the maximum incorporation of KR_9C into PFTD monolayers at pH 3, 5, and 8. Red and green lines represent the $\Delta\Phi^m$ and Π^m_0 at which the maximum was reached.

We conclude this section with a secondary but nonetheless relevant observation. Arginine molecules in solution, with a concentration equivalent to KR_9C 10 μM, neither incorporate into the partially ionized MA monolayer nor to the fully ionized PFTD film (both at pH 5 and Π_0 = 10 mN/m). This supports the idea that increasing the chain length of polyarginines, within

DOI: 10.1021/acs.langmuir.7b04038
Langmuir XXXX, XXX, XXX−XXX

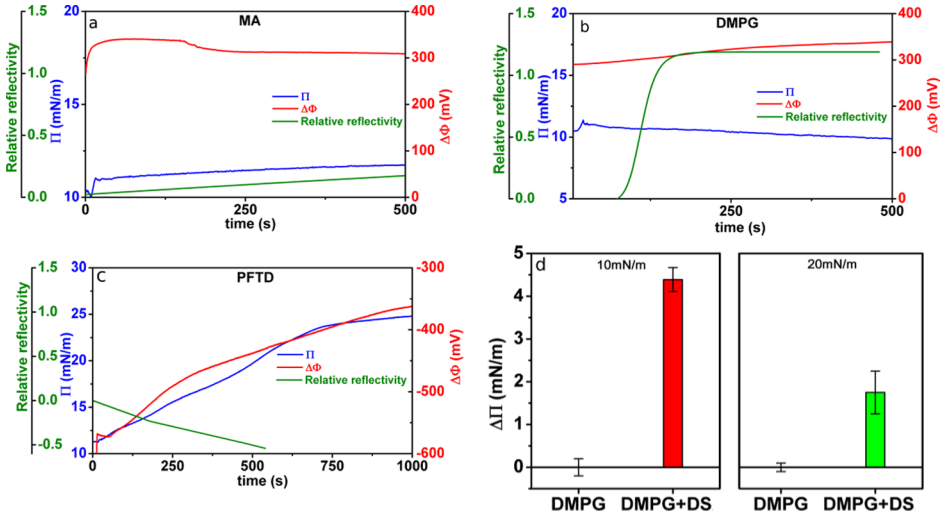

Figure 4. Time evolution of surface pressure (Π, blue), surface potential (ΔΦ, red), and relative reflectivity (green) for (a) MA, (b) DMPG, and (c) PFTD monolayers, at pH 5 and Π_0 = >10 mN/m. (d) Surface pressure change after injecting KR_9C in the subphase underneath a DMPG monolayer in the presence and in the absence of a DS sublayer, at initial surface pressures of 10 mN/m (red) and 20 mN/m (green). The data correspond to the average of three independent experiments ± SD.

certain margins, fosters the incorporation of the peptide into membranes.[44]

Carboxylate Moieties Favor CPP Incorporation into Lipid Monolayers. The results of the previous section highlight the relevance of a charged polar head group and of a negative dipole potential on the incorporation of KR_9C into fatty acid monolayers. However, at the light of the claim that carboxylate moieties favor the membrane translocation of polycationic peptides,[21] it is important to check whether this is a generic effect, associated, for example, to the resulting membrane surface charge, or it is specific of the fatty acids or molecules alike.

To probe the role of carboxylates on CPP adsorption and membrane insertion, we contrasted the experiments discussed in the previous section with equivalent essays performed on DMPG monolayers. In the latter case, the pH of the subphase was set to 5, guaranteeing the complete ionization of the film.[45] DMPG monolayers provide a negatively charged film but do not exhibit a carboxylate moiety, which allows for testing the influence of the charge in the absence of the COO^- peptide chelator. It has to be recalled, however, that DMPG contains a phosphate group, which has also been proposed as a chelator of the guanidinium group,[21,22] and seems to be more efficient than fatty acids for extracting oligoarginines to an organic phase.[22] Besides, it has been shown that the presence of phosphatidylglycerol (PG) lipids in phosphatidylcholine (PC) membranes favors the penetration of CPP into monolayers[46,47] and vesicles of different sizes.[12,48−54]

To our surprise, KR_9C did not show evidence of incorporation into the DMPG film, as indicated by ΔΠ, at any of the initial surface pressures investigated (see Figure S9). However, the lack of change in surface pressure does not rule out the possibility that the CPP is still binding to the polar head groups of the amphiphiles while remaining on the aqueous side of the interface.[55] To explore such a scenario, we registered simultaneously the time evolution of the surface pressure and the reflectivity of the monolayer, and in another set of experiments also the surface potential, after the peptide was injected under monolayers sustained at 10 mN/m. In general, the reflectivity of an interface increases as the film thickness increases,[35] which provides a qualitative measurement of the accumulation of material beneath the film. Figure 4a−c shows the results for monolayers made of MA, DMPG, or PFTD at pH 5.

Although the reflectivity of the MA films did not change significantly upon peptide injection, a sharp increase was observed in the DMPG monolayer and a decrease in the PFTD monolayer. On the contrary, the surface potential increased in all systems, with the largest changes observed in PFTD. The behavior of MA is not very surprising considering that, at pH 5 and Π_0 10 mN/m, the peptide has relatively little effect on surface pressure of this film (Figure 1). On the other side, the trend depicted by DMPG indicates that the peptide, in spite of not incorporating into the film, accumulates under the monolayer, increasing the interface reflectivity as previously observed for cationic and anionic polymers,[55] and slightly increasing the surface potential. Figure 5 shows a schematic representation of the adsorption of KR_9C beneath a DMPG monolayer. We can therefore conclude that a negatively charged surface promotes the surface binding, or adsorption, of the CPP; but that the incorporation of the peptide into the film involves further requirements, which seem to be propitiated by molecules with a carboxylic acid moiety.

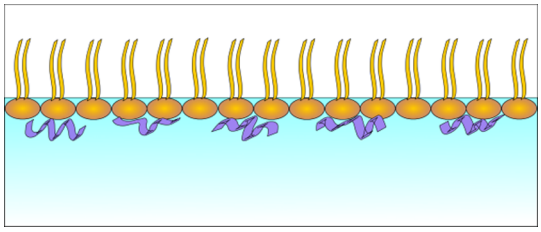

Figure 5. Illustration of how KR_9C (violet) accumulates beneath the DMPG film (yellow). The actual structure of the peptide at the interface is unknown, and the drawings are schematic.

The reduction in reflectivity depicted by PFTD may seem surprising, but it can be readily explained considering that the reflectivity of fluorinated monolayers decreases with the film density,[30] as opposed to the trends observed in hydrogenated

DOI: 10.1021/acs.langmuir.7b04038
Langmuir XXXX, XXX, XXX−XXX

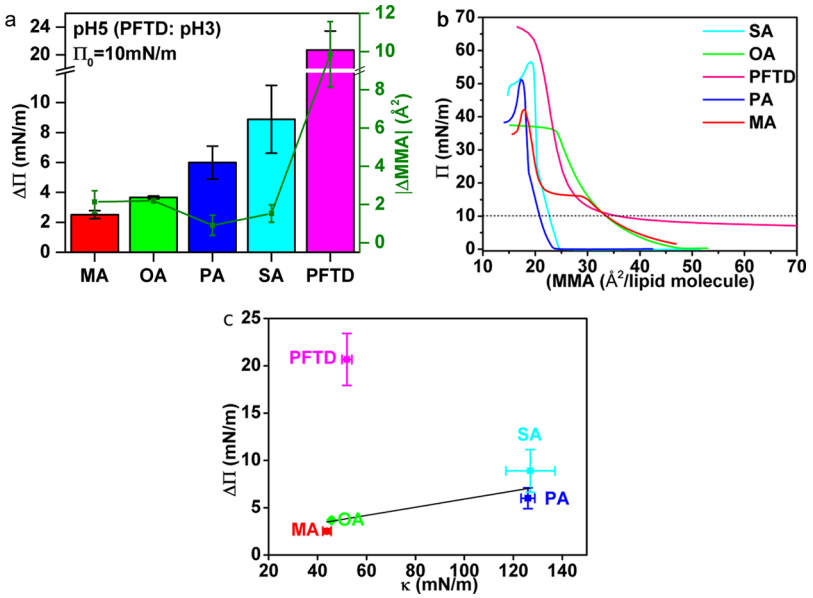

Figure 6. Interaction of KR_9C with monolayers of MA (red), OA (green), PA (blue), SA (cyan), and PFTD (pink). (a) ΔΠ induced by KR_9C in monolayers at Π_0 = 10 mN/m. The green line represents the (absolute) variation in mean molecular area for each lipid because of the incorporation of the peptide. (b) Compression isotherms of the analyzed lipids. (c) ΔΠ induced by KR_9C plotted as a function of the compressibility modulus of the pure lipid monolayers at 10 mN/m (i.e., the initial surface pressure set in the penetration experiments). All experiments were carried out at T = 25 °C and pH 5, except for PFTD that were performed at pH 3.

lipids. Therefore, the decrease in PFTD reflectivity is a direct consequence of the increment in film density induced by the incorporation of the peptide. At the same time, the change in surface potential in this system is more pronounced than in the other two cases because the monolayer initially shows a negative surface potential, leading to larger changes after the incorporation of the positively charged CPP.

It has also been proved that the presence of negatively charged glycosaminoglycans favors the cellular intake of CPP, by increasing the peptide concentration near the cell surface.[56−59] To test the effect of this kind of polymers on the incorporation of KR_9C into DMPG monolayers, lipid films were prepared onto solutions of DS, an anionic polysaccharide that in the presence of $CaCl_2$ (10 mM) forms a polymeric sublayer under the film,[55] simulating glycosaminoglycans. Under such experimental conditions, a slight increase in the surface pressure of DMPG was detected after injecting the CPP (Figure 4d), but the effect was still smaller than in the case of ionized fatty acid monolayers (pH 8 Figure 1, for example). Therefore, we can conclude that KR_9C incorporates substantially into partially and completely ionized MA, PA, and PFTD monolayers, but only slightly into anionic DMPG monolayers, when supplemented with an anionic polymeric sublayer. On one side, these conclusions support the idea that carboxylated lipids facilitate the passive diffusion of CPP across bilayers. On the other side, it also suggests that in DMPG monolayers, the PO_3^{2-} ligands are shielded by the hydrated glycerol moiety.

It is important to notice that our results do not contradict the widely reported increment in CPP permeation in vesicles containing PG lipids.[18,19,60] Negatively charged PGs simply increase the surface concentration of the peptide, that in turn promotes activated jumps across the membrane. Schwieger et al.[64] have also observed the incorporation of polyarginines into 1,2-dipalmitoyl-*sn*-glycero-3-phosphatidylglycerol monolayers, but the peptide they tested was much longer than KR_9C. Also, our results do not oppose those of Sakai et al.,[22] mentioned before, because in those experiments the CPP binds to DMPG molecules dispersed in a chloroformic solution (biphasic extraction system), instead of forming an ordered membrane. On the contrary, here the PG lipids form a well-ordered monolayer with highly hydrated polar head groups. Our results, however, appear to disagree with those of Alhakamy et al. who showed that nonarginine (10 μM) incorporated into 1-palmitoyl-2-oleoyl-*sn*-glycero-3-phosphatidylglycerol (POPG) monolayers generate a surface pressure change of about 4 mN/m.[46] This discrepancy could be ascribed to the unsaturation of POPG, which promotes disorder in the monolayer lattice, probably affecting the head groups region. This observation highlights how important is the accessibility of the phosphate group in PGs, which in turn can be modulated by the hydrocarbon chains. In fact, the modulating effect of the hydrophobic tails was reported by Alhakamy for PC lipids: although nonarginine generates a 2 mN/m increment in the surface pressure of POPC monolayers, DPPC did not show any change. We will not go deeper into this effect because we are more interested in the carboxylate moiety than in the phosphate group, but further experiments on this issue would be valuable.

Because our results show that ionized carboxylic acids favor the insertion of CPP into monolayers, we tested other fatty acids with the aim of generalizing our observations and to analyze the effect of the hydrocarbon chain on the kinetics of insertion.

Role of Hydrophobic Chains on the Interaction of CPP with Fatty Acid Monolayers. To test the influence of the hydrophobic chains on the insertion of KR_9C, two fatty acids were added to the analysis. We studied monolayers made of OA, as an example of unsaturated lipid, and of SA, a lipid that forms solid films. These experiments were carried out at pH 5, at which the amphiphiles are partially dissociated and all of them form stable monolayers. Figure 6a compares the change in surface pressure promoted by the incorporation of the

DOI: 10.1021/acs.langmuir.7b04038
Langmuir XXXX, XXX, XXX−XXX

peptide at Π_0 = 10 mN/m. Because $\Delta\Pi$ depends both on the amount of peptide incorporated and on the stiffness of the monolayer (i.e., the pressure response of the film because of a change in the area per lipid), we estimated the change in the mean area occupied by the lipids upon incorporation of the peptide, ΔA. The resulting data (in absolute values) are presented in Figure 6a.

Considering that the total area of the monolayer remains constant during the measurement of a penetration curve, ΔA was estimated assuming that the film can be tessellated into two types of regions. The first ones are defined by regions where the peptide penetrates and disrupts the monolayer structure, forming a lipid−peptide aggregate. The second ones are formed by pure lipids. According to this model, the pure lipid regions get progressively compressed as the peptide penetrates and the peptide−lipid aggregate is formed. ΔA corresponds then to the change in the area per lipid, within the pure lipid regions, which can be estimated from the mean molecular areas at the final and initial surface pressures, as read from the compression isotherms of the pure monolayers (Figure 6b). A 2 Å^2 change in area was determined when the peptide was incorporated into monolayers of hydrogenated fatty acids, which corresponds to ∼6% change in the global area. This is a very small percent of change; thus, it validates the assumption of a tessellated monolayer, in which regions of pure lipid persist.

Figure 6a shows that, although $\Delta\Pi$ increases in the order MA ≤ OA < PA ≤ SA < PFTD, the values of ΔA are similar for all the hydrogenated fatty acids. Therefore, the trend in $\Delta\Pi$ is a consequence of the phase state of the monolayers at Π_0 = 10 mN: MA and OA are in the liquid-expanded state, whereas PA and SA are present in a solid state (Figure 6b). To better quantify this observation, we correlated $\Delta\Pi$ with the compressibility modulus, κ, of the pure lipid films at 10 mN/m. The results are shown in Figure 6c. $\Delta\Pi$ increases with κ for the hydrogenated fatty acids, whereas the fluorinated lipid shows a large $\Delta\Pi$, despite its low compressibility, that correlates with a high value of ΔA.

All in all, we can conclude that the most influential parameter in the incorporation of KR_9C into hydrogenated fatty acid monolayers is the carboxylate moiety, rather than the lipid density. This explains the little influence of the initial surface pressure on $\Delta\Pi$, as observed in Figure 1. Furthermore, Figure 6c highlights the fact that the negative surface potential of PFTD promotes the membrane incorporation of KR_9C to a larger extend than in any of the hydrogenated fatty acids.

Judging from the values of ΔA, all of the hydrogenated fatty acids absorb similar amounts of CPP into the monolayer. However, the kinetics of peptide insertion depends on the length of the hydrophobic chain. Figure 7 shows the time at which the CPP produces half the maximum $\Delta\Pi$ ($t_{1/2}$, red columns), together with the *lag time*, which is the time elapsed since the peptide injection until the surface pressure starts increasing. These kinetic parameters are indicated in Figure S10 for a schematic penetration curve. Our results show a clear slowdown in the kinetics of peptide insertion as the chain length of the lipid increases. The two C14 fatty acids show the shortest $t_{1/2}$ and no lag time, within the time resolution of our experiments. Conversely, monolayers of the saturated and unsaturated C18 acids responded more slowly to the incorporation of KR_9C and showed larger lag times. These results suggest that the rate of CPP insertion into a flat lipid structure is dominated by the reorganization of the hydrocarbon chains, with higher energy barriers for longer chains.

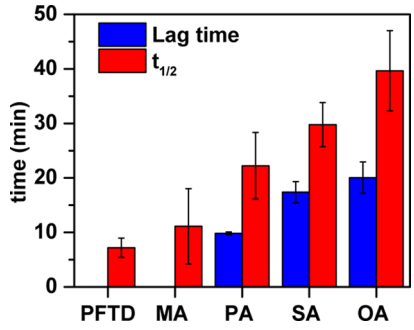

Figure 7. Lag time and $t_{1/2}$ values associated with the kinetics of incorporation of KR_9C into films of PFTD, MA, PA, SA, and OA. See Figure S10 for a graphical definition of *lag time* and $t_{1/2}$. The data correspond to the average of three independent experiments ± SD.

At the light of the previous discussion, we hypothesize that a peptide−lipid aggregate may form between KR_9C and the carboxylic moieties, as sketched in Figure 8.

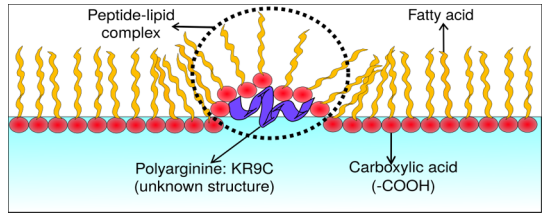

Figure 8. Illustration of the peptide−lipid aggregate formed between KR_9C (violet) and carboxylic moieties accumulates beneath the DMPG film (yellow). The actual structure of the peptide at the interface is unknown and the drawings are schematic.

CONCLUSIONS

In this paper, we have characterized the binding and insertion of a cell-penetrating peptide, KR_9C, into lipid monolayers. Three main conclusions can be drawn from our study. First, the penetration of the peptide into fatty acid monolayers is regulated by the pH of the subphase, as it partially controls the charge density of the monolayer. Anionic films are more prone to interact with polycationic CPP, as previously reported for different model membranes.[46,61] However, the surface charge density is not the only relevant parameter. We have shown that the carboxylate functional group fosters the polyarginine insertion probably because it is a good ligand for the guanidinium group of arginine, which is present in large amounts in almost all CPP. These results agree with the observation that fatty acids can sequestrate CPP from an aqueous solution.[21] The salient role of carboxylates was gauged by comparing the insertion of the peptide into DMPG and fatty acid monolayers at the intermediate pH. Although KR_9C was adsorbed onto DMPG, it was not inserted into the lipid structure. It could be argued that the DMPG monolayer had a lower charge density that any of the fatty acid monolayers because the mean molecular area of DMPG is larger. However, it has to be recalled that the incorporation of KR_9C into MA occurred even at pH 5, where the monolayer is only partially ionized. Moreover, our results should not be interpreted as a complete absence of specific interactions between phosphate and guanidinium groups because it has been previously shown that KR_9C incorporates into PC monolayers.[62] More suitably, our results suggest that the balance of specific (hydrogen-

DOI: 10.1021/acs.langmuir.7b04038
Langmuir XXXX, XXX, XXX−XXX

bonding) and nonspecific interactions (electrostatics and van der Waals) is different for fatty acids and PG monolayers. Electrostatic forces may be similar in both cases, but the carboxylate moiety of fatty acids is able to chelate the guanidinium group, forming a peptide−lipid aggregate at the interface, whereas the phosphate group of DMPG is less accessible to the peptide on the aqueous side of the interphase.

Second, a negative dipole potential favors the incorporation of the peptide into the monolayer, counterbalancing the negative effect of the increased film density in perfluorinated fatty acids. It could be argued that the larger insertion affinity of KR_9C for PFTD, in comparison with PA, is not because of a negative dipole potential but because of the fact that PFTD forms softer monolayers. However, even considering those differences in mechanical properties, the effects on surface pressure and area changes, as shown in Figure 6, are larger for PFTD than that for PA monolayers. Favorable partition of anions relative to cations is largely known from experiments with hydrogenated lipid bilayers. This is explained by considering that the positive dipole potential of each hemilayer generates an electrostatic environment more favorable to anions than cations.[43] Analogously, in the present work, we show that films formed by molecules that bear negative dipole potentials are prone to cation insertion than those with positive potentials.

Third, we tested whether the phase state of the monolayer or the hydrocarbon chain length further regulated the absorption of the peptide into fatty acid monolayers. Our results show that the area of the film perturbed by the penetration of the peptide (when forming a lipid−peptide aggregate) is similar in all tested hydrogenated fatty acids, being the kinetic of penetration-dependent on the hydrocarbon chain length. It might be surprising that the incorporation process does not depend on the monolayer stiffness because it is commonly observed (and it is also expected) that stiff monolayers are less prone to absorb molecules from solution. However, the result shown in Figure 6 agrees with the very low slope of the $\Delta\Pi$ versus Π_0 plots. Therefore, we conclude that the penetration of KR_9C into fatty acid monolayers is not prevented by their high degree of compactness. Even more, the energy barrier for CPP insertion is not larger in stiff monolayers than in soft monolayers, suggesting that the formation of a stable peptide−lipid structure pays the energy cost for the overall compression of the monolayer ($\Delta\Pi > 0$), making the whole process favorable even for highly close-packed films.

In summary, as suggested in Figure 8, we propose that CPP forms a tight complex with carboxylic acids, leading to the rearrangement of the lipids' hydrocarbon chains. Our results suggest that these peptide−lipid aggregates have a well-defined peptide−carboxylic acid proportion, independently of the length of the fatty acid. Such complex does not form with unpolymerized arginine residues because the control experiments with Arg (R) 90 μM induced no increase in the surface pressure of the fatty acid films. Thus, a polyarginine chain seems to be necessary for the formation of a stable guanidinium−carboxylate complex. The energy cost of such a rearrangement is larger to the longer the hydrocarbon chains, which is a determining factor of the CPP insertion kinetics. Our results support some of the ideas behind the so-called adaptive translocation mechanism[63] for CPP permeation. Such a mechanism proposes that the peptide gets tightly associated to a certain number of lipid molecules, which carry the CPP across the membrane while masking its electrical charge and rendering the whole process energetically favorable. Here, we show that this kind of peptide−lipid aggregate are able to form with KR_9C in monolayers composed of fatty acids.

■ ASSOCIATED CONTENT

Supporting Information

The Supporting Information is available free of charge on the ACS Publications website at DOI: 10.1021/acs.langmuir.7b04038.

Doses-response curve for KR9C; compression isotherms and surface potential of PFTD; compression isotherms and surface potential of MA monolayers; compression isotherms and surface potential of PA monolayers; time evolution of the surface pressure after injection of KR9C under PFTD monolayers; DP vs pH for MA, PA, and PFTD; dependence of the transition pressure with pH for a PFTD monolayer; surface potential for a PFTD monolayer at P0 = 10 mN/m and 20 mN/m; time evolution of the surface pressure after injection of KR9C under DMPG films; and time evolution of the surface pressure after injection of KR9C under a PFTD film (PDF)

■ AUTHOR INFORMATION

Corresponding Author

*E-mail: wilke@mail.fcq.unc.edu.ar. Phone: +54-351-5353855. Fax: +54-351-5353855.

ORCID

Natalia Wilke: 0000-0002-2342-0193

Notes

The authors declare no competing financial interest.

■ ACKNOWLEDGMENTS

This work was supported by SECyT-UNC, CONICET and FONCYT (Program BID, grants PICT 2012-0344 and PICT 2012-2759) Argentina. N.W. and M.G.D.P. are Career Investigators and M.A.V. is a fellow of CONICET. M.G.D.P. and M.A.V. also thank SECTyP-UNCUYO and EU Commission Marie Curie RISE ENACT Programme (643998).

■ REFERENCES

(1) Heitz, F.; Morris, M. C.; Divita, G. Twenty years of cell-penetrating peptides: from molecular mechanisms to therapeutics. *Br. J. Pharmacol.* **2009**, *157*, 195−206.

(2) Zorko, M.; Langel, Ü. Cell-penetrating peptides: mechanism and kinetics of cargo delivery. *Adv. Drug Delivery Rev.* **2005**, *57*, 529−545.

(3) Di Pisa, M.; Chassaing, G.; Swiecicki, J.-M. Translocation Mechanism(s) of Cell-Penetrating Peptides: Biophysical Studies Using Artificial Membrane Bilayers. *Biochemistry* **2015**, *54*, 194−207.

(4) Shin, M. C.; Zhang, J.; Min, K. A.; Lee, K.; Byun, Y.; David, A. E.; He, H.; Yang, V. C. Cell-penetrating peptides: Achievements and challenges in application for cancer treatment. *J. Biomed. Mater. Res., Part A* **2014**, *102*, 575−587.

(5) Hoyer, J.; Neundorf, I. Peptide Vectors for the Nonviral Delivery of Nucleic Acids. *Acc. Chem. Res.* **2012**, *45*, 1048−1056.

(6) Zappavigna, S.; Misso, G.; Falanga, A.; Perillo, E.; Novellino, E.; Galdiero, M.; Grieco, P.; Caraglia, M.; Galdiero, S. Nanocarriers Conjugated with Cell Penetrating Peptides: New Trojan Horses by Modern Ulysses. *Curr. Pharm. Biotechnol.* **2016**, *17*, 700−722.

(7) Mussbach, F.; Franke, M.; Zoch, A.; Schaefer, B.; Reissmann, S. Transduction of peptides and proteins into live cells by cell penetrating peptides. *J. Cell. Biochem.* **2011**, *112*, 3824−3833.

DOI: 10.1021/acs.langmuir.7b04038
Langmuir XXXX, XXX, XXX−XXX

(8) Dinca, A.; Chien, W.-M.; Chin, M. T. Intracellular Delivery of Proteins with Cell-Penetrating Peptides for Therapeutic Uses in Human Disease. *Int. J. Mol. Sci.* **2016**, *17*, 263.
(9) Farkhani, S. M.; Valizadeh, A.; Karami, H.; Mohammadi, S.; Sohrabi, N.; Badrzadeh, F. Cell penetrating peptides: Efficient vectors for delivery of nanoparticles, nanocarriers, therapeutic and diagnostic molecules. *Peptides* **2014**, *57*, 78−94.
(10) El-Andaloussi, S.; Holm, T.; Langel, U. Cell-Penetrating Peptides: Mechanisms and Applications. *Curr. Pharm. Des.* **2005**, *11*, 3597.
(11) Kauffman, W. B.; Fuselier, T.; He, J.; Wimley, W. C. Mechanism Matters: A Taxonomy of Cell Penetrating Peptides. *Trends Biochem. Sci.* **2015**, *40*, 749−764.
(12) Thorén, P. E. G.; Persson, D.; Esbjörner, E. K.; Goksör, M.; Lincoln, P.; Nordén, B. Membrane Binding and Translocation of Cell-Penetrating Peptides. *Biochemistry* **2004**, *43*, 3471−3489.
(13) Lin, J.; Alexander-Katz, A. Cell Membranes Open Doors for Cationic Nanoparticles/Biomolecules: Insights into Uptake Kinetics. *ACS Nano* **2013**, *7*, 10799−10808.
(14) Sani, M.-A.; Separovic, F. How Membrane-Active Peptides Get into Lipid Membranes. *Acc. Chem. Res.* **2016**, *49*, 1130−1138.
(15) Pujals, S.; Fernández-Carneado, J.; López-Iglesias, C.; Kogan, M. J.; Giralt, E. Mechanistic aspects of CPP-mediated intracellular drug delivery: Relevance of {CPP} self-assembly. *Biochim. Biophys. Acta, Biomembr.* **2006**, *1758*, 264−279.
(16) Morris, M. C.; Deshayes, S.; Heitz, F.; Divita, G. Cell-penetrating peptides: from molecular mechanisms to therapeutics. *Biol. Cell* **2008**, *100*, 201−217.
(17) Rothbard, J.; Jessop, T.; Wender, P. Adaptive translocation: the role of hydrogen bonding and membrane potential in the uptake of guanidinium-rich transporters into cells. *Adv. Drug Delivery Rev.* **2005**, *57*, 495−504.
(18) Terrone, D.; Sang, S. L. W.; Roudaia, L.; Silvius, J. R. Penetratin and Related Cell-Penetrating Cationic Peptides Can Translocate Across Lipid Bilayers in the Presence of a Transbilayer Potential. *Biochemistry* **2003**, *42*, 13787−13799.
(19) Sharmin, S.; Islam, M. Z.; Karal, M. A. S.; Shibly, S. U. A.; Dohra, H.; Yamazaki, M. Effects of Lipid Composition on the Entry of Cell-Penetrating Peptide Oligoarginine into Single Vesicles. *Biochemistry* **2016**, *55*, 4154−4165.
(20) Swiecicki, J.-M.; Bartsch, A.; Tailhades, J.; Di Pisa, M.; Heller, B.; Chassaing, G.; Mansuy, C.; Burlina, F.; Lavielle, S. The Efficacies of Cell-Penetrating Peptides in Accumulating in Large Unilamellar Vesicles Depend on their Ability To Form Inverted Micelles. *ChemBioChem* **2014**, *15*, 884−891.
(21) Herce, H. D.; Garcia, A. E.; Cardoso, M. C. Fundamental Molecular Mechanism for the Cellular Uptake of Guanidinium-Rich Molecules. *J. Am. Chem. Soc.* **2014**, *136*, 17459−17467.
(22) Sakai, N.; Takeuchi, T.; Futaki, S.; Matile, S. Direct Observation of Anion-Mediated Translocation of Fluorescent Oligoarginine Carriers into and across Bulk Liquid and Anionic Bilayer Membranes. *ChemBioChem* **2005**, *6*, 114−122.
(23) Bechara, C.; Sagan, S. Cell-penetrating peptides: 20 years later, where do we stand? *FEBS Lett.* **2013**, *587*, 1693−1702.
(24) Koren, E.; Torchilin, V. P. Cell-penetrating peptides: breaking through to the other side. *Trends Mol. Med.* **2012**, *18*, 385−393.
(25) El-Sayed, A.; Futaki, S.; Harashima, H. Delivery of Macromolecules Using Arginine-Rich Cell-Penetrating Peptides: Ways to Overcome Endosomal Entrapment. *AAPS J.* **2009**, *11*, 13−22.
(26) Chugh, A.; Eudes, F.; Shim, Y.-S. Cell-penetrating peptides: Nanocarrier for macromolecule delivery in living cells. *IUBMB Life* **2010**, *62*, 183−193.
(27) Ruzza, P.; Biondi, B.; Marchiani, A.; Antolini, N.; Calderan, A. Cell-Penetrating Peptides: A Comparative Study on Lipid Affinity and Cargo Delivery Properties. *Pharmaceuticals* **2010**, *3*, 1045−1062.
(28) Vogel, V.; Möbius, D. Local surface potentials and electric dipole moments of lipid monolayers: Contributions of the water/lipid and the lipid/air interfaces. *J. Colloid Interface Sci.* **1988**, *126*, 408−420.
(29) Brockman, H. Dipole potential of lipid membranes. *Chem. Phys. Lipids* **1994**, *73*, 57−79.
(30) Broniatowski, M.; Dynarowicz-Łątka, P. Langmuir monolayers from perfluorobutyl-n-eicosane. *J. Fluorine Chem.* **2004**, *125*, 1501−1507.
(31) Schwarz, G.; Taylor, S. E. Thermodynamic Analysis of the Surface Activity Exhibited by a Largely Hydrophobic Peptide. *Langmuir* **1995**, *11*, 4341−4346.
(32) Schwarz, G.; Taylor, S. E. Peptide-lipid interactions in Langmuir monolayers at the air/water interface. A novel thermodynamic analysis of a two-component surfactant system. *Supramol. Sci.* **1997**, *4*, 479−483.
(33) Gaines, G. L., Jr. *Insoluble monolayer at liquid-gas interfaces*; Interscience Publishers, 1966; p 233
(34) Betts, J. J.; Pethica, B. A. The ionization characteristics of monolayers of weak acids and bases. *Trans. Faraday Soc.* **1956**, *52*, 1581−1589.
(35) Wilke, N. *Advances in Planar Lipid Bilayers and Liposomes*; Elsevier Science BV, 2014; pp 51−81.
(36) Wilke, N. *Comprehensive guide for nanocoatings technology*; NOVA Science, 2015; pp 139−158.
(37) Mercado, F. V.; Maggio, B.; Wilke, N. Phase diagram of mixed monolayers of stearic acid and dimyristoylphosphatidylcholine. Effect of the acid ionization. *Chem. Phys. Lipids* **2011**, *164*, 386−392.
(38) Maget-Dana, R. The monolayer technique: a potent tool for studying the interfacial properties of antimicrobial and membrane-lytic peptides and their interactions with lipid membranes. *Biochim. Biophys. Acta, Biomembr.* **1999**, *1462*, 109−140.
(39) Varas, M.; Sánchez-Borzone, M.; Sánchez, J. M.; de Barioglio, S. R.; Perillo, M. A. Surface Behavior and PeptideLipid Interactions of the Cyclic Neuropeptide Melanin Concentrating Hormone. *J. Phys. Chem. B* **2008**, *112*, 7330−7337.
(40) Ambroggio, E. E.; Separovic, F.; Bowie, J.; Fidelio, G. D. Surface behaviour and peptidelipid interactions of the antibiotic peptides, Maculatin and Citropin. *Biochim. Biophys. Acta, Biomembr.* **2004**, *1664*, 31−37.
(41) Pedrera, L.; Gomide, A. B.; Sánchez, R. E.; Ros, U.; Wilke, N.; Pazos, F.; Lanio, M. E.; Itri, R.; Fanani, M. L.; Alvarez, C. The Presence of Sterols Favors Sticholysin I-Membrane Association and Pore Formation Regardless of Their Ability to Form Laterally Segregated Domains. *Langmuir* **2015**, *31*, 9911−9923.
(42) Demel, R. A.; van Kessel, W. S. M. G.; Zwaal, R. F. A.; Roelofsen, B.; van Deenen, L. L. M. Relation between various phospholipase actions on human red cell membranes and the interfacial phospholipid pressure in monolayers. *Biochim. Biophys. Acta, Biomembr.* **1975**, *406*, 97−107.
(43) Clarke, R. J. The dipole potential of phospholipid membranes and methods for its detection. *Adv. Colloid Interface Sci.* **2001**, *89*−*90*, 263−281.
(44) Mitchell, D. J.; Steinman, L.; Kim, D. T.; Fathman, C. G.; Rothbard, J. B. Polyarginine enters cells more efficiently than other polycationic homopolymers. *J. Pept. Res.* **2000**, *56*, 318−325.
(45) Ramos, A. P.; Pavani, C.; Iamamoto, Y.; Zaniquelli, M. E. D. Porphyrinphospholipid interaction and ring metallation depending on the phospholipid polar head type. *J. Colloid Interface Sci.* **2010**, *350*, 148−154.
(46) Alhakamy, N. A.; Kaviratna, A.; Berkland, C. J.; Dhar, P. Dynamic Measurements of Membrane Insertion Potential of Synthetic Cell Penetrating Peptides. *Langmuir* **2013**, *29*, 15336−15349.
(47) Alhakamy, N. A.; Elandaloussi, I.; Ghazvini, S.; Berkland, C. J.; Dhar, P. Effect of Lipid Headgroup Charge and pH on the Stability and Membrane Insertion Potential of Calcium Condensed Gene Complexes. *Langmuir* **2015**, *31*, 4232−4245.
(48) He, X.; Lin, M.; Guo, J.; Qu, Z.; Xu, F. Experimental and simulation studies of polyarginines across the membrane of giant unilamellar vesicles. *RSC Adv.* **2016**, *6*, 30454−30459.
(49) Jobin, M.-L.; Blanchet, M.; Henry, S.; Chaignepain, S.; Manigand, C.; Castano, S.; Lecomte, S.; Burlina, F.; Sagan, S.; Alves, I. D. The role of tryptophans on the cellular uptake and membrane

DOI: 10.1021/acs.langmuir.7b04038
Langmuir XXXX, XXX, XXX−XXX

interaction of arginine-rich cell penetrating peptides. *Biochim. Biophys. Acta, Biomembr.* **2015**, *1848*, 593−602.
(50) Walrant, A.; Vogel, A.; Correia, I.; Lequin, O.; Olausson, B. E. S.; Desbat, B.; Sagan, S.; Alves, I. D. Membrane interactions of two arginine-rich peptides with different cell internalization capacities. *Biochim. Biophys. Acta, Biomembr.* **2012**, *1818*, 1755−1763.
(51) Reuter, M.; Schwieger, C.; Meister, A.; Karlsson, G.; Blume, A. Poly-l-lysines and poly-l-arginines induce leakage of negatively charged phospholipid vesicles and translocate through the lipid bilayer upon electrostatic binding to the membrane. *Biophys. Chem.* **2009**, *144*, 27−37.
(52) Bouchet, A. M.; Lairion, F.; Ruysschaert, J.-M.; Lensink, M. F. Oligoarginine vectors for intracellular delivery: Role of arginine side-chain orientation in chain length-dependent destabilization of lipid membranes. *Chem. Phys. Lipids* **2012**, *165*, 89−96.
(53) Takechi, Y.; Tanaka, H.; Kitayama, H.; Yoshii, H.; Tanaka, M.; Saito, H. Comparative study on the interaction of cell-penetrating polycationic polymers with lipid membranes. *Chem. Phys. Lipids* **2012**, *165*, 51−58.
(54) Lamazière, A.; Maniti, O.; Wolf, C.; Lambert, O.; Chassaing, G.; Trugnan, G.; Ayala-Sanmartin, J. Lipid domain separation, bilayer thickening and pearling induced by the cell penetrating peptide penetratin. *Biochim. Biophys. Acta, Biomembr.* **2010**, *1798*, 2223−2230.
(55) Cámara, C. I.; Wilke, N. Interaction of dextran derivatives with lipid monolayers and the consequential modulation of the film properties. *Chem. Phys. Lipids* **2017**, *204*, 34−42.
(56) Schmidt, N.; Mishra, A.; Lai, G. H.; Wong, G. C. L. Arginine-rich cell-penetrating peptides. *FEBS Lett.* **2010**, *584*, 1806−1813.
(57) Gonçalves, E.; Kitas, E.; Seelig, J. Binding of Oligoarginine to Membrane Lipids and Heparan Sulfate: Structural and Thermodynamic Characterization of a Cell-Penetrating Peptide. *Biochemistry* **2005**, *44*, 2692−2702.
(58) Ziegler, A.; Li Blatter, X.; Seelig, A.; Seelig, J. Protein Transduction Domains of HIV-1 and SIV TAT Interact with Charged Lipid Vesicles. Binding Mechanism and Thermodynamic Analysis. *Biochemistry* **2003**, *42*, 9185−9194.
(59) Ziegler, A. Thermodynamic studies and binding mechanisms of cell-penetrating peptides with lipids and glycosaminoglycans. *Adv. Drug Delivery Rev.* **2008**, *60*, 580−597.
(60) Islam, M. Z.; Ariyama, H.; Alam, J. M.; Yamazaki, M. Entry of Cell-Penetrating Peptide Transportan 10 into a Single Vesicle by Translocating Across Lipid Membrane and Its Induced Pores. *Biochemistry* **2014**, *53*, 386−396.
(61) Eiríksdóttir, E.; Konate, K.; Langel, Ü.; Divita, G.; Deshayes, S. Secondary structure of cell-penetrating peptides controls membrane interaction and insertion. *Biochim. Biophys. Acta, Biomembr.* **2010**, *1798*, 1119−1128.
(62) Via, M.; Klug, J.; Wilke, N.; Mayorga, L. S.; Del Pópolo, M. G. Interfacial electrostatic potential modulates the insertion of cell-penetrating-peptides into lipid bilayers. *Phys. Chem. Chem. Phys.* **2018**, *20*, 5180−5189.
(63) Alves, I.; Walrant, A.; Bechara, C.; Sagan, S. Is There Anybody in There? On The Mechanisms of Wall Crossing of Cell Penetrating Peptides. *Curr. Protein Pept. Sci.* **2012**, *13*, 658−671.
(64) Schwieger, C.; Blume, A. Interaction of Poly(l-arginine) with Negatively Charged DPPG Membranes: Calorimetric and Monolayer Studies. *Biomacromolecules* **2009**, *10* (8), 2152−2161.

DOI: 10.1021/acs.langmuir.7b04038
Langmuir XXXX, XXX, XXX−XXX